Functional Consequences of Splicing of the Antisense Transcript COOLAIR on FLC Transcription

Marquardt, S., Raitskin, O., Wu, Z., Liu, F., Sun, Q., & Dean, C. (2014). Functional Consequences of Splicing of the Antisense Transcript COOLAIR on FLC Transcription. DOI: 10.1016/j.molcel.2014.03.026

Published in:
Molecular Cell

Document Version:
Publisher's PDF, also known as Version of record

Queen's University Belfast - Research Portal:
Link to publication record in Queen's University Belfast Research Portal

Molecular Cell
Article

Functional Consequences of Splicing of the Antisense Transcript *COOLAIR* on *FLC* Transcription

Sebastian Marquardt,[1,2] Oleg Raitskin,[1] Zhe Wu,[1] Fuquan Liu,[1,3] Qianwen Sun,[1] and Caroline Dean[1,*]
[1]Department of Cell & Developmental Biology, John Innes Centre, Norwich Research Park, Norwich NR4 7UH, UK
[2]Present address: Department of Biological Chemistry and Molecular Pharmacology, Harvard Medical School, Boston, MA 02115, USA
[3]Present address: Institute of Global Food Security, School of Biological Sciences, Queen's University, Belfast, BT9 7BL, UK
*Correspondence: caroline.dean@jic.ac.uk
http://dx.doi.org/10.1016/j.molcel.2014.03.026

SUMMARY

Antisense transcription is widespread in many genomes; however, how much is functional is hotly debated. We are investigating functionality of a set of long noncoding antisense transcripts, collectively called *COOLAIR,* produced at *Arabidopsis FLOWERING LOCUS C* (*FLC*). *COOLAIR* initiates just downstream of the major sense transcript poly(A) site and terminates either early or extends into the *FLC* promoter region. We now show that splicing of *COOLAIR* is functionally important. This was revealed through analysis of a hypomorphic mutation in the core spliceosome component PRP8. The *prp8* mutation perturbs a cotranscriptional feedback mechanism linking *COOLAIR* processing to *FLC* gene body histone demethylation and reduced *FLC* transcription. The importance of *COOLAIR* splicing in this repression mechanism was confirmed by disrupting *COOLAIR* production and mutating the *COOLAIR* proximal splice acceptor site. Our findings suggest that altered splicing of a long noncoding transcript can quantitatively modulate gene expression through cotranscriptional coupling mechanisms.

INTRODUCTION

The biological significance of non-protein-coding genomic sequences has been an issue for decades (Britten and Davidson, 1969; Mattick, 2004). This has recently been reinforced by the finding that most of the human genome is represented in primary transcripts (Djebali et al., 2012). The majority of these are long, spliced, and polyadenylated RNA Polymerase II (RNA Pol II) transcripts, and a large number are antisense transcripts to annotated genes (Derrien et al., 2012; Osato et al., 2007; Lehner et al., 2002; Lu et al., 2012; Wang et al., 2005; Yamada et al., 2003). Many of the long (>200 nt) noncoding RNAs show no evolutionary conservation, adding to the debate of whether they serve any function (Gerstein et al., 2012; Graur et al., 2013).

Several in-depth studies in yeast have shown that noncoding transcripts have the potential to regulate gene expression through transcriptional interference or recruitment of chromatin modifiers (Camblong et al., 2007; Hongay et al., 2006; Castelnuovo et al., 2013). However, roles of noncoding transcripts in higher eukaryotes are less well understood. Some have been shown to play roles in chromatin regulation (Wang and Chang, 2011), although it can be the transcriptional overlap rather than the antisense transcript itself that is important for the functional consequence (Latos et al., 2012).

We have focused on the functional consequences of antisense transcription through our study of the regulation of *Arabidopsis FLOWERING LOCUS C* (*FLC*) gene, a developmental regulator that controls the timing of the switch to reproductive development. *FLC* encodes a MADS box transcriptional regulator that represses flowering, and *FLC* expression quantitatively correlates with flowering time (Sheldon et al., 1999; Michaels and Amasino, 1999). There are several regulatory pathways that converge to regulate *FLC*: two that antagonistically regulate *FLC* in ambient temperatures—the FRIGIDA pathway, which activates *FLC* expression, and the autonomous pathway, which downregulates *FLC*—and one more, vernalization, which epigenetically silences *FLC* in response to prolonged cold (Figure 1A). All of these pathways involve a set of antisense transcripts, collectively named as *COOLAIR*, that fully encompass the *FLC* gene, initiating immediately downstream of the sense strand polyadenylation site and terminating beyond the sense transcription start site (Hornyik et al., 2010; Liu et al., 2010; Swiezewski et al., 2009). *COOLAIR* transcripts are polyadenylated at multiple sites with proximal polyadenylation promoted by components of the autonomous promotion pathway. These include the RNA-binding proteins FCA and FPA, the 3′ processing factors Cstf64, Cstf77 and FY, the CPSF component and homolog of yeast Pfs2p and mammalian WDR33 (Liu et al., 2010; Ohnacker et al., 2000; Simpson et al., 2003). Use of the proximal poly(A) site results in quantitative downregulation of *FLC* expression in a process requiring FLD, an H3K4me2 demethylase (Liu et al., 2010). FLD activity results in H3K4me2 demethylation in the gene body of *FLC* and transcriptional downregulation of *FLC* (Liu et al., 2007, 2010). Loss of any of the autonomous pathway components reduces usage of the proximal polyadenylation site, which leads to increased *FLC* transcription. Analysis of the regulation of *COOLAIR* transcription has recently identified an RNA-DNA heteroduplex, or R-loop, covering the *COOLAIR* promoter (Sun et al., 2013). Stabilization of this R-loop by a novel homeodomain protein limits

COOLAIR transcription, adding another layer of regulation within the autonomous pathway.

We have continued to investigate the transcriptional circuitry at *FLC* and how *COOLAIR* is linked to changes in *FLC* expression. Here, through identification of a hypomorphic mutation in the core spliceosome component PRP8, we reveal how *COOLAIR* functionally modulates *FLC* gene expression through

in *prp8-6*; if anything, there was an elevated level (Figure S3D). A similar lack of effect of *prp8-6* was observed on expression of other autonomous pathway components (Figure S3E); thus, we concluded that the increase of *FLC* expression by *prp8-6* is unlikely to be due to an indirect effect on autonomous pathway function.

Various polymorphisms have been reported between the *FLC* alleles of the Col and L*er* laboratory strains (*Col-FLC* and L*er-FLC*), including the presence of a Mutator transposon at the 3′ end of intron 1 (Liu et al., 2004). As *FLC-LUC* is based on *Col-FLC*, we tested the effect of *prp8-6* on both alleles in the same samples by northern blotting using an *FLC* probe that discriminates by size. We detected only two transcript species reflecting L*er-FLC* and *FLC* (*Col*)*-LUC* in *prp8-6,* both of which were increased compared to the progenitor (Figure 2A). We therefore concluded that the *prp8-6*-induced increase in expression is independent of the *cis* polymorphism between these two *FLC* alleles. We also analyzed flowering time and established that *prp8-6* delays flowering (

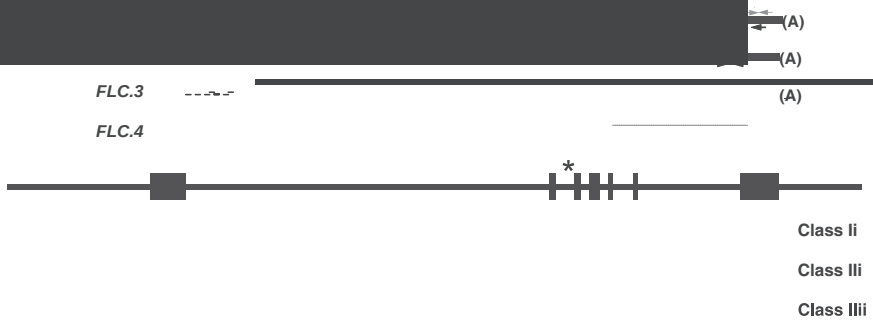

C

sites (primers shown in Table S1). *prp8-6* reduced usage of the *COOLAIR* proximal poly(A) site and promoted use of the distal site (Figure 4A). Northern blot analysis showed these data are representative of poly(A) site usage of *COOLAIR* transcripts

gene insertions and avoid the issue of between transgenic line expression variability. *prp8-6* did not lead to any further increases in expression in combination with *FLC*^{tex}. This epistasis is consistent with loss of *COOLAIR* production and *prp8-6* influ-

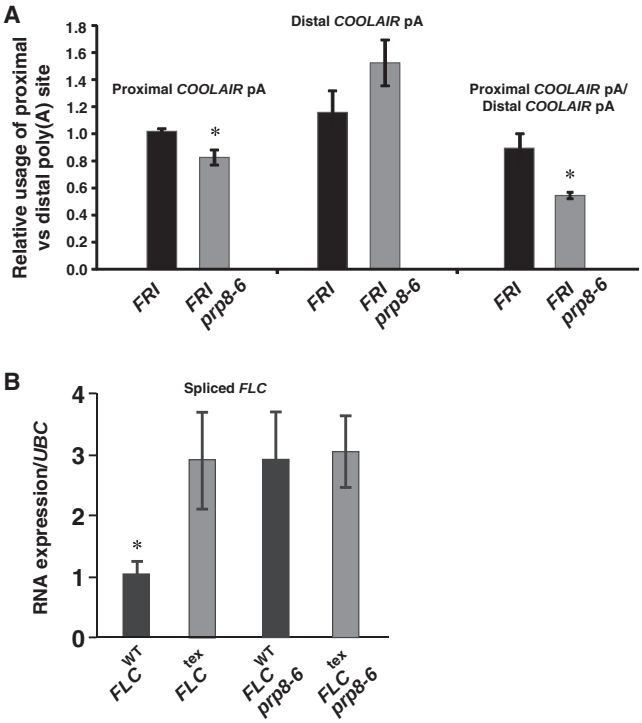

Figure 4. *COOLAIR* Plays a Role in *FLC*-Mediated Repression by PRP8

(A) Relative usage of a proximal and distal poly(A) sites of *COOLAIR* in *prp8-6*. Proximal and distal poly(A) site usage was assessed by qRT-PCR, as described in Supplemental Experimental Procedures, using primers listed in Table S1 and expressed as relative to total *COOLAIR*. Genotypes are indicated as *FRI* wild-type (black) and *FRI prp8-6* mutants (gray). Values are means from three biological repeats ±SEM.

(B) Three representative FLC^{tex} transgenic lines and two *FLC* genomic DNA transgenic controls were crossed to *prp8-6* and genotypes homozygous for *prp8-6* and all T-DNAs identified. RNA was pooled from each genotype to obtain an average expression value. Averages qRT-PCR values from three independent pooling experiments ±SEM are shown.

(A and B) Student's t test was performed. p values <0.05 are denoted by (*). See also Figure S5.

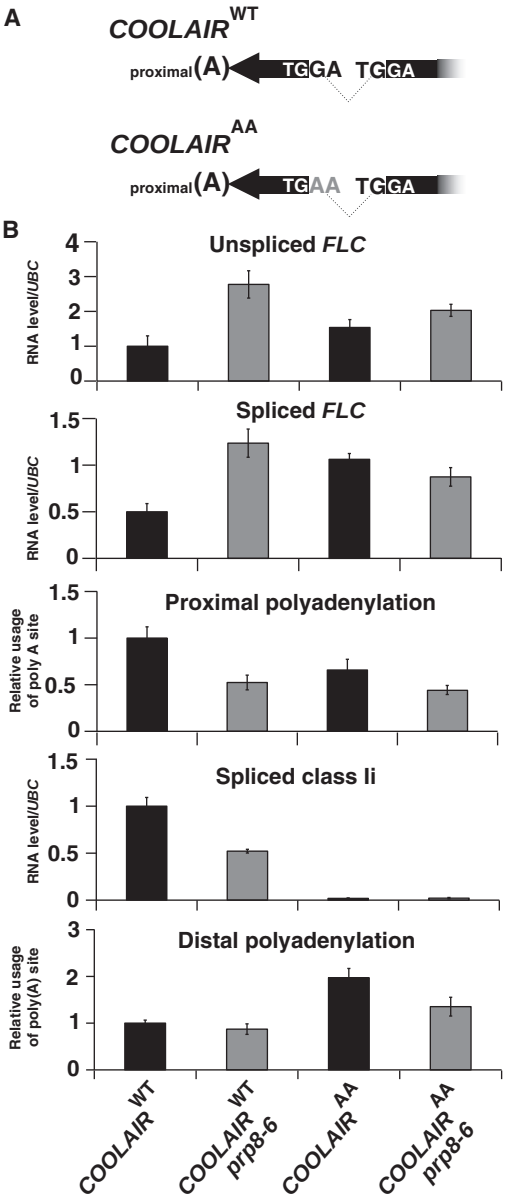

Figure 5. Mutation of *COOLAIR* Intron 1 Splice Acceptor Site Disrupts PRP8-Dependent Regulation of *FLC* Expression

(A) Schematic representation of intron 1 junction sequence in the wild-type transcript ($COOLAIR^{WT}$) or at the mutated 3′ splice site ($COOLAIR^{AA}$).

(B) qRT-PCR analysis of *FLC* unspliced and spliced RNA and relative levels of the different *COOLAIR* forms in the different transgenic genotypes. Ten to fifteen independent transgenic lines for each genotype were harvested and analyzed in pools; values are means ±SEM. qRT-PCR was used to analyze transcript levels relative to UBC. For unspliced, spliced, proximal polyadenylation, and spliced class1i, the $COOLAIR^{WT}$ value was significantly different ($p < 0.05$) from the other three genotypes. For distal polyadenylation, the $COOLAIR^{AA}$ mean is significantly higher than that of $COOLAIR^{WT}$ ($p < 0.05$). See also Figure S6.

intron. Often when the AG dinucleotide at the end of an intron is mutated downstream, AG dinucleotides are utilized instead. We used PCR with flanking primers, but we did not detect other splicing events (Figure S6A). Proximal poly(A) site usage of *COOLAIR* was reduced, and this was not additive to the *prp8-6*-induced changes (Figures 5B). Overall, these data support the view that the *prp8-6* phenotypic effects are smaller than many other autonomous pathway mutants but involve reduced splicing of *COOLAIR* class Ii intron, which reduces *COOLAIR* proximal poly(A) site usage.

Coupling of Splicing, Chromatin State, and Transcriptional Level

Alternative polyadenylation of the *COOLAIR* transcripts has been shown to trigger changes in histone methylation, increased transcription as assayed by unspliced transcript production, and RNA Pol II occupancy at the *FLC* locus (Liu et al., 2007, 2010). We therefore analyzed whether *prp8-6* influenced H3K4 demethylation and Pol II occupancy at *FLC*. *prp8-6* increased H3K4me2 in the body of the gene downstream of the proximal *COOLAIR* poly(A) site (Figures 6A and S6B), similar to changes

induced by *fld* and *fca* mutations (Liu et al., 2007). We addressed whether these changes were mediated through FLD, the H3K4me2 demethylase involved in *FLC* downregulation. Consistent with a connection between PRP8 activity and FLD-induced H3K4me2 demethylation, we found that combination of the hypomorphic *prp8-6* allele with a weak *fld* mutation led to a synergistic effect on *FLC* derepression (Figure S7A). As with *fca* and *fld* mutants, the increase in H3K4me2 in *prp8-6* was associated with increased Pol II occupancy (Figures 6B, S6C, and S6D). These data support a model whereby efficient splicing of class Ii intron via PRP8 activity promotes proximal poly(A) site choice in the antisense transcript via FCA, FY activity. In turn, this proximal polyadenylation triggers FLD-mediated H3K4me2 demethylation in the gene body, which restrains transcription of *FLC*.

We then investigated how splicing and polyadenylation of *COOLAIR* might be coupled with the chromatin state at *FLC* in two ways. First, we analyzed *COOLAIR* splicing and polyadenylation in the *fld* demethylase mutant. The splicing efficiency of antisense introns class Ii was significantly reduced in *fld*, as in *fca* (Figures 6C and 6D). In addition, proximal poly(A) site usage was reduced (Figure 6E) and distal poly(A) site usage increased (Figure 6F) in an *fld* mutant. This suggested that there was positive feedback between the chromatin state at *FLC* and alternative *COOLAIR* splicing and polyadenylation. Second, we analyzed seedlings treated with the histone deacetylase inhibitor trichostatin A in order to increase the acetylation level of *FLC* chromatin. This was stimulated by the observation that *fld* mutations result in hyperacetylation of histones in *FLC* chromatin (He et al., 2003). As expected, transcriptional activity at the locus assayed by *FLC* unspliced RNA increased (Figure 7A). This was associated with an increase in total *COOLAIR* production (Figure 7B), consistent with previous data of a positive correlation between total *FLC* and total *COOLAIR* production (Swiezewski et al., 2009), and a relative reduction in proximally polyadenylated *COOLAIR* (Figure 7C). This further supported a positive feedback mechanism coupling chromatin state with *COOLAIR* processing. Chromatin modification has been proposed to affect transcript processing indirectly through influencing transcription elongation rate (Alló et al., 2009). If this is the case here, it is not dependent on the transcriptional pause release factor TFIIS (Grasser et al., 2009), because *tfIIs* mutations do not influence *COOLAIR* poly(A) site choice (Figures S7B–S7D).

DISCUSSION

The functional importance of long noncoding RNAs is a major issue in molecular biology. Analysis of the control of flowering time has enabled us to address this issue by investigating the roles of a set of long noncoding transcripts, collectively called *COOLAIR,* produced at the *Arabidopsis* locus *FLC*. *FLC* encodes a repressor of flowering whose expression level determines whether plants over-winter before flowering. Here, analysis of a hypomorphic mutation in the essential PRP8 spliceosomal subunit suggests a role for *COOLAIR* splicing in the quantitative modulation of *FLC* transcription. This hypomorphic mutation is likely to reveal the sensitivity of *FLC* regulation to changes in general function gene regulators, rather than particular specificity in PRP8 targets. Genetic and molecular analysis revealed that

FLC regulators both developmentally and environmentally has previously been documented. For example, one of the components of the autonomous pathway, FCA, is itself subject to negative autoregulation via alternative polyadenylation with maximal expression in the shoot and root apical meristem not reached until 5 days after germination (Macknight et al., 1997). Temperature influences several of the autonomous and FRIGIDA pathway functions (Jung et al., 2012; Blázquez et al., 2003). All these influences could then modulate the dynamics of the feedback loop so quantitatively modulating *FLC* transcription. The cotranscriptional mechanism regulating expression of the floral repressor gene *FLC* is revealing concepts of general importance to gene regulation.

EXPERIMENTAL PROCEDURES

Trans-Complementation of *sof81* with the Genomic *PRP8*

The genomic region encompassing the *PRP8*/*SUS2* gene on *Arabidopsis* chromosome I was inserted into a TAC library cosmid clone (pJATY50P17) that was available through the John Innes Genome Centre. A 10 kb genomic *PRP8* region was amplified by PCR with the oligonucleotides PRP8-SacII-SbfI-F and PRP8-KpnI-R using pJATY50P17 as template with Phusion DNA polymerase (NEB). The PCR fragment was cloned into the binary plant transformation vector *pCambia-1300*, conferring hygromycin resistance in plants via SbfI/KpnI cloning to generate ASM4. The cloned genomic *PRP8* region in ASM4 was sequenced to verify the absence of mutations. ASM4 was transformed into *sof81* mutants by *Agrobacterium* mediated floral-dip transformation, and hygromycin-resistant T1 transformants were isolated (n > 10). The activity of the FLC-LUC reporter of the transformants was compared to untransformed *sof81* mutant controls.

Cloning of *FLC*, *COOLAIR*^{AA}, and *COOLAIR*^{TEX}

FLC was cloned as a genomic SacI fragment (~12 kb) into the *Arabidopsis* binary vector *pCambia-1300*, which confers hygromycin resistance in plants. To generate *COOLAIR*^{AA}, fragments F1 (1,325 bp) and F2 (311 bp) were amplified from *FLC* with primers for F1 (FLC3ss_F1-forward and FLC3ss_F1-reverse) and F2 (FLC3ss_F2-forward and FLC3ss_F2- reverse) containing a mutated sequence for the 3′ splice site of *FLC* antisense class Ii intron (AA instead of AG). PCR amplification was performed with Phusion polymerase (NEB). Resulting fragments F1 and F2 with overlapping ends were fused together in 1:1 molar ratio by PCR amplification with Phusion polymerase (NEB) employing the forward primer for F1 and the reverse primer for F2. The resulting fragment was digested with NheI and BglII, gel purified, and subsequently cloned into an SphI fragment of *FLC*, replacing the wild-type NheI-BglII fragment. The resulting SphI fragment with the mutated class Ii antisense 3′ splice site was inserted into *FLC-pCambia-1300*. This mutation creates a recognition site for DraI (TTTAAA), which has been used for genotyping the hygromycin resistant transformants to verify presence of the *COOLAIR*^{AA} mutation.

F2 homozygotes of the following genotypes: *prp8-6/flc-2/FRI* and *PRP8/flc-2/FRI* were obtained from crosses of *prp8-6* and *flc-2/FRI*. The F2 homozygotes were transformed using *Agrobacterium*-mediated transformation of floral buds with the either *FLC-pCambia-1300* or *COOLAIR*^{AA}*-pCambia-1300*. The seeds from a total of 49 T1 (first generation) transformants (13 plants of *COOLAIR*^{AA}*/PRP8/flc-2/FRI*, 11 plants of *COOLAIR*^{AA}*/prp8-6/flc-2/FRI*, 15 plants of *FLC/PRP8/flc-2/FRI* and 10 plants of *FLC/prp8-6/flc-2/FRI*) were sown on GM medium without glucose and selected for hygromycin resistance (T2 generation). RNA for analysis was extracted from 4-week old seedlings.

For cloning *COOLAIR*^{TEX}, the sequence TAGCCACC that contains *FLC* translational stop TAG codon was mutagenized to create EheI restriction site TGGCGCCC. A SspI-SspI fragment containing the strong *RBCS* terminator (706 bp) was PCR amplified and cloned in sense direction between EheI and SwaI restriction sites (SwaI is located 741 bp downstream of the *FLC* stop codon, therefore replacing the corresponding genomic sequence of 3′ UTR of *FLC* and flanking downstream region to create *COOLAIR*^{TEX}).

To analyze the effect of *FLC*^{tex} seeds were collected from four homozygous plants of *FLC*^{tex}*/flc-2/prp8-6/FRI* and five homozygous plants of *FLC*^{tex}*/flc-2/PRP8/FRI*. These plants were obtained from the three independent crosses of *FLC*^{tex}*/flc-2/FRI to prp8-6/Ler*. As a control for the *FLC*^{tex} analysis, the *flc-2/FRI* plants were transformed with *pSLJ-FLC*15 (10 kg clone of Columbia *FLC* gene) and crossed with *prp8-6/Ler* (two independent crosses). Three plants from either *FLC/flc-2/prp8-6/FRI* or *FLC/flc-2/PRP8/FRI* were obtained. The seedlings from *FLC*^{tex} and corresponding *pSLJ-FLC* transgenic plants were grown on GM medium without glucose and BASTA resistant transformants were isolated for analysis.

Measuring *FLC* Sense Transcript

For the sense *FLC* mRNA analysis, reverse transcription was performed using *FLC* specific reverse primers with SuperScript®III Reverse Transcriptase (Invitrogen). qPCR analysis was performed on LightCycler480®II (ROCHE) with primers FLC Unspliced_LP and FLC Unspliced_RP for the unspliced sense *FLC* transcript and with primers FLC Spliced_LP and FLC Spliced_RP for the spliced sense *FLC* transcript. qPCR data was normalized to *UBC* (which was amplified with primers UBC-F and UBC-R). The primers are described in Table S1.

Measuring *COOLAIR* Splicing Efficiency

To measure the splicing efficiency of class Ii intron, 5 μg of total RNA isolated from seedlings were reverse-transcribed into cDNA, primed by Int1_RT, which is located in the exon 2 of class I and class II ii, (for locations of the primers, see also the illustration presented in Figure 3A). Resulting cDNA was used as template in qPCR reactions to amplify cDNA with the first small intron spliced by primers Int1_spliced_LP and Int1_spliced_RP, which covers the splicing junction. cDNA with the first small unspliced intron was amplified by primers Int1_unspliced_LP and Int1_unspliced_RP, which is located in the first small intron. Triplicates of all PCR reactions were performed and quantified against standard curves of cDNA dilutions. These data were then used to calculate the mean together with the spliced/unspliced ratio. RT− controls were always included to confirm absence of genomic DNA contamination.

To measure *COOLAIR* class II intron splicing efficiency, 5 μg of total RNA isolated from seedlings was reverse-transcribed into cDNA, primed by Class II unspliced F, and located in the last exon of all the class II antisense RNA. The resulting cDNA was used as template in qPCR to amplify spliced class II i with primers Class II-1_LP and Class II-1_RP, which cover the splicing junction; Class II ii intron 2 spliced with primers Class II-2_LP and Class II-2_RP, which cover the splicing junction; and *FLC* antisense big introns unspliced with primers Class II unspliced F and Class II unspliced R. Triplicate PCR reactions were performed and quantified against standard curves of cDNA dilutions before calculating the mean and spliced/unspliced ratio. RT− controls were always included to confirm absence of genomic DNA contamination.

Measuring Polyadenylated *COOLAIR*

The following primers were employed for the analysis of the *COOLAIR* transcripts: (a) for proximal poly(A) site transcript oligo(dT) primer was used for the reverse transcription and forward primer, set1_RP, and reverse primer, LP_FLCin6polyA, used for the qPCR analysis (Liu et al., 2010), and (b) for the distal poly(A) site, oligo(dT) primer was used for the reverse transcription and forward primer Set4_RP and reverse primer Set4_LP used for the qPCR analysis. qPCR reactions were performed in triplicates for each sample. Average values of the triplicates were normalized to the expression of total COOLAIR (which was amplified with Total *COOLAIR*_LP and Total COOLAIR_RP primers). The primers are summarized in the Table S1.

SUPPLEMENTAL INFORMATION

Supplemental Information includes seven figures, one table, and Supplemental Experimental Procedures and can be found with this article online at http://dx.doi.org/10.1016/j.molcel.2014.03.026.

ACKNOWLEDGMENTS

We thank all members of the Dean group for discussions. This research was supported by a EU Marie Curie PhD studentship to S.M. (MEST-CT-2005-019727), a Marie Curie Fellowship to O.R., and European Research Council Advanced Investigator (233039 ENVGENE) and BBSRC BB/D010799/1 grants to C.D.

Received: September 30, 2013
Revised: December 22, 2013
Accepted: March 4, 2014
Published: April 10, 2014

REFERENCES

Ali, G.S., Palusa, S.G., Golovkin, M., Prasad, J., Manley, J.L., and Reddy, A.S. (2007). Regulation of plant developmental processes by a novel splicing factor. PLoS ONE *2*, e471.

Alló, M., Buggiano, V., Fededa, J.P., Petrillo, E., Schor, I., de la Mata, M., Agirre, E., Plass, M., Eyras, E., Elela, S.A., et al. (2009). Control of alternative splicing through siRNA-mediated transcriptional gene silencing. Nat. Struct. Mol. Biol. *16*, 717–724.

Batsché, E., Yaniv, M., and Muchardt, C. (2006). The human SWI/SNF subunit Brm is a regulator of alternative splicing. Nat. Struct. Mol. Biol. *13*, 22–29.

Blázquez, M.A., Ahn, J.H., and Weigel, D. (2003). A thermosensory pathway controlling flowering time in *Arabidopsis thaliana*. Nat. Genet. *33*, 168–171.

Britten, R.J., and Davidson, E.H. (1969). Gene regulation for higher cells: a theory. Science *165*, 349–357.

Bumgarner, S.L., Neuert, G., Voight, B.F., Symbor-Nagrabska, A., Grisafi, P., van Oudenaarden, A., and Fink, G.R. (2012). Single-cell analysis reveals that noncoding RNAs contribute to clonal heterogeneity by modulating transcription factor recruitment. Mol. Cell *45*, 470–482.

Camblong, J., Iglesias, N., Fickentscher, C., Dieppois, G., and Stutz, F. (2007). Antisense RNA stabilization induces transcriptional gene silencing via histone deacetylation in *S. cerevisiae*. Cell *131*, 706–717.

Castelnuovo, M., Rahman, S., Guffanti, E., Infantino, V., Stutz, F., and Zenklusen, D. (2013). Bimodal expression of *PHO84* is modulated by early termination of antisense transcription. Nat. Struct. Mol. Biol. *20*, 851–858.

de la Mata, M., Alonso, C.R., Kadener, S., Fededa, J.P., Blaustein, M., Pelisch, F., Cramer, P., Bentley, D., and Kornblihtt, A.R. (2003). A slow RNA polymerase II affects alternative splicing in vivo. Mol. Cell *12*, 525–532.

Derrien, T., Johnson, R., Bussotti, G., Tanzer, A., Djebali, S., Tilgner, H., Guernec, G., Martin, D., Merkel, A., Knowles, D.G., et al. (2012). The GENCODE v7 catalog of human long noncoding RNAs: analysis of their gene structure, evolution, and expression. Genome Res. *22*, 1775–1789.

Djebali, S., Davis, C.A., Merkel, A., Dobin, A., Lassmann, T., Mortazavi, A., Tanzer, A., Lagarde, J., Lin, W., Schlesinger, F., et al. (2012). Landscape of transcription in human cells. Nature *489*, 101–108.

Galej, W.P., Oubridge, C., Newman, A.J., and Nagai, K. (2013). Crystal structure of Prp8 reveals active site cavity of the spliceosome. Nature *493*, 638–643.

Gerstein, M.B., Kundaje, A., Hariharan, M., Landt, S.G., Yan, K.K., Cheng, C., Mu, X.J., Khurana, E., Rozowsky, J., Alexander, R., et al. (2012). Architecture of the human regulatory network derived from ENCODE data. Nature *489*, 91–100.

Grainger, R.J., and Beggs, J.D. (2005). Prp8 protein: at the heart of the spliceosome. RNA *11*, 533–557.

Grasser, M., Kane, C.M., Merkle, T., Melzer, M., Emmersen, J., and Grasser, K.D. (2009). Transcript elongation factor TFIIS is involved in *arabidopsis* seed dormancy. J. Mol. Biol. *386*, 598–611.

Graur, D., Zheng, Y., Price, N., Azevedo, R.B., Zufall, R.A., and Elhaik, E. (2013). On the immortality of television sets: ''function'' in the human genome according to the evolution-free gospel of ENCODE. Genome Biol. Evol. *5*, 578–590.

Greb, T., Mylne, J.S., Crevillen, P., Geraldo, N., An, H., Gendall, A.R., and Dean, C. (2007). The PHD finger protein VRN5 functions in the epigenetic silencing of *Arabidopsis FLC*. Curr. Biol. *17*, 73–78.

Hazelbaker, D.Z., Marquardt, S., Wlotzka, W., and Buratowski, S. (2013). Kinetic competition between RNA Polymerase II and Sen1-dependent transcription termination. Mol. Cell *49*, 55–66.

He, Y., Michaels, S.D., and Amasino, R.M. (2003). Regulation of flowering time by histone acetylation in *Arabidopsis*. Science *302*, 1751–1754.

Hongay, C.F., Grisafi, P.L., Galitski, T., and Fink, G.R. (2006). Antisense transcription controls cell fate in *Saccharomyces cerevisiae*. Cell *127*, 735–745.

Hornyik, C., Terzi, L.C., and Simpson, G.G. (2010). The spen family protein FPA controls alternative cleavage and polyadenylation of RNA. Dev. Cell *18*, 203–213.

Johanson, U., West, J., Lister, C., Michaels, S., Amasino, R., and Dean, C. (2000). Molecular analysis of FRIGIDA, a major determinant of natural variation in *Arabidopsis* flowering time. Science *290*, 344–347.

Jung, J.H., Seo, P.J., Ahn, J.H., and Park, C.M. (2012). *Arabidopsis* RNA-binding protein FCA regulates microRNA172 processing in thermosensory flowering. J. Biol. Chem. *287*, 16007–16016.

Kornblihtt, A.R., Schor, I.E., Alló, M., Dujardin, G., Petrillo, E., and Muñoz, M.J. (2013). Alternative splicing: a pivotal step between eukaryotic transcription and translation. Nat. Rev. Mol. Cell Biol. *14*, 153–165.

Latos, P.A., Pauler, F.M., Koerner, M.V., Şenergin, H.B., Hudson, Q.J., Stocsits, R.R., Allhoff, W., Stricker, S.H., Klement, R.M., Warczok, K.E., et al. (2012). Airn transcriptional overlap, but not its lncRNA products, induces imprinted Igf2r silencing. Science *338*, 1469–1472.

Lehner, B., Williams, G., Campbell, R.D., and Sanderson, C.M. (2002). Antisense transcripts in the human genome. Trends Genet. *18*, 63–65.

Liu, M.M., and Zack, D.J. (2013). Alternative splicing and retinal degeneration. Clin. Genet. *84*, 142–149.

Liu, J., He, Y.H., Amasino, R., and Chen, X.M. (2004). siRNAs targeting an intronic transposon in the regulation of natural flowering behavior in *Arabidopsis*. Genes Dev. *18*, 2873–2878.

Liu, F., Quesada, V., Crevillén, P., Bäurle, I., Swiezewski, S., and Dean, C. (2007). The *Arabidopsis* RNA-binding protein FCA requires a lysine-specific demethylase 1 homolog to downregulate *FLC*. Mol. Cell *28*, 398–407.

Liu, M., Yuan, L., Liu, N.Y., Shi, D.Q., Liu, J., and Yang, W.C. (2009). GAMETOPHYTIC FACTOR 1, involved in pre-mRNA splicing, is essential for megagametogenesis and embryogenesis in *Arabidopsis*. J. Integr. Plant Biol. *51*, 261–271.

Liu, F., Marquardt, S., Lister, C., Swiezewski, S., and Dean, C. (2010). Targeted 3′ processing of antisense transcripts triggers *Arabidopsis FLC* chromatin silencing. Science *327*, 94–97.

Liu, F., Bakht, S., and Dean, C. (2012). Cotranscriptional role for *Arabidopsis* DICER-LIKE 4 in transcription termination. Science *335*, 1621–1623.

Lu, T., Zhu, C., Lu, G., Guo, Y., Zhou, Y., Zhang, Z., Zhao, Y., Li, W., Lu, Y., Tang, W., et al. (2012). Strand-specific RNA-seq reveals widespread occurrence of novel cis-natural antisense transcripts in rice. BMC Genomics *13*, 721.

Macknight, R., Bancroft, I., Page, T., Lister, C., Schmidt, R., Love, K., Westphal, L., Murphy, G., Sherson, S., Cobbett, C., and Dean, C. (1997). FCA, a gene controlling flowering time in *Arabidopsis*, encodes a protein containing RNA-binding domains. Cell *89*, 737–745.

Martincic, K., Alkan, S.A., Cheatle, A., Borghesi, L., and Milcarek, C. (2009). Transcription elongation factor ELL2 directs immunoglobulin secretion in plasma cells by stimulating altered RNA processing. Nat. Immunol. *10*, 1102–1109.

Martinson, H.G. (2011). An active role for splicing in 3′-end formation. Wiley Interdiscip. Rev. RNA *2*, 459–470.

Mattick, J.S. (2004). RNA regulation: a new genetics? Nat. Rev. Genet. *5*, 316–323.

Michaels, S.D., and Amasino, R.M. (1999). *FLOWERING LOCUS C* encodes a novel MADS domain protein that acts as a repressor of flowering. Plant Cell *11*, 949–956.

Mozaffari-Jovin, S., Santos, K.F., Hsiao, H.H., Will, C.L., Urlaub, H., Wahl, M.C., and Lührmann, R. (2012). The Prp8 RNase H-like domain inhibits Brr2-mediated U4/U6 snRNA unwinding by blocking Brr2 loading onto the U4 snRNA. Genes Dev. *26*, 2422–2434.

Ohnacker, M., Barabino, S.M., Preker, P.J., and Keller, W. (2000). The WD-repeat protein pfs2p bridges two essential factors within the yeast pre-mRNA 3′-end-processing complex. EMBO J. *19*, 37–47.

Osato, N., Suzuki, Y., Ikeo, K., and Gojobori, T. (2007). Transcriptional interferences in cis natural antisense transcripts of humans and mice. Genetics *176*, 1299–1306.

Pena, V., Rozov, A., Fabrizio, P., Lührmann, R., and Wahl, M.C. (2008). Structure and function of an RNase H domain at the heart of the spliceosome. EMBO J. *27*, 2929–2940.

Quesada, V., Macknight, R., Dean, C., and Simpson, G.G. (2003). Autoregulation of FCA pre-mRNA processing controls *Arabidopsis* flowering time. EMBO J. *22*, 3142–3152.

Saint-André, V., Batsché, E., Rachez, C., and Muchardt, C. (2011). Histone H3 lysine 9 trimethylation and HP1γ favor inclusion of alternative exons. Nat. Struct. Mol. Biol. *18*, 337–344.

Schwartz, B.W., Yeung, E.C., and Meinke, D.W. (1994). Disruption of Morphogenesis and Transformation of the Suspensor in Abnormal Suspensor Mutants of *Arabidopsis*. Development *120*, 3235–3245.

Sheldon, C.C., Burn, J.E., Perez, P.P., Metzger, J., Edwards, J.A., Peacock, W.J., and Dennis, E.S. (1999). The *FLF* MADS box gene: a repressor of flowering in *Arabidopsis* regulated by vernalization and methylation. Plant Cell *11*, 445–458.

Simpson, G.G., Dijkwel, P.P., Quesada, V., Henderson, I., and Dean, C. (2003). FY is an RNA 3′ end-processing factor that interacts with FCA to control the *Arabidopsis* floral transition. Cell *113*, 777–787.

Sonmez, C., Bäurle, I., Magusin, A., Dreos, R., Laubinger, S., Weigel, D., and Dean, C. (2011). RNA 3′ processing functions of *Arabidopsis* FCA and FPA limit intergenic transcription. Proc. Natl. Acad. Sci. USA *108*, 8508–8513.

Sun, Q., Csorba, T., Skourti-Stathaki, K., Proudfoot, N.J., and Dean, C. (2013). R-loop stabilization represses antisense transcription at the *Arabidopsis FLC* locus. Science *340*, 619–621.

Swiezewski, S., Liu, F., Magusin, A., and Dean, C. (2009). Cold-induced silencing by long antisense transcripts of an *Arabidopsis* Polycomb target. Nature *462*, 799–802.

Wang, K.C., and Chang, H.Y. (2011). Molecular mechanisms of long noncoding RNAs. Mol. Cell *43*, 904–914.

Wang, X.J., Gaasterland, T., and Chua, N.H. (2005). Genome-wide prediction and identification of cis-natural antisense transcripts in *Arabidopsis thaliana*. Genome Biol. *6*, R30.

Wang, C., Tian, Q., Hou, Z., Mucha, M., Aukerman, M., and Olsen, O.A. (2007). The *Arabidopsis thaliana* AT PRP39-1 gene, encoding a tetratricopeptide repeat protein with similarity to the yeast pre-mRNA processing protein PRP39, affects flowering time. Plant Cell Rep. *26*, 1357–1366.

Yamada, K., Lim, J., Dale, J.M., Chen, H., Shinn, P., Palm, C.J., Southwick, A.M., Wu, H.C., Kim, C., Nguyen, M., et al. (2003). Empirical analysis of transcriptional activity in the *Arabidopsis* genome. Science *302*, 842–846.

Zhang, Y., Zhang, X.-O., Chen, T., Xiang, J.-F., Yin, Q.-F., Xing, Y.-H., Zhu, S., Yang, L., and Chen, L.L. (2013). Circular intronic long noncoding RNAs. Mol. Cell *51*, 792–806.